

# SYNTHESIS OF CONTROLLERS FOR THE ACTIVE MASS DRIVER SYSTEM IN THE PRESENCE OF UNCERTAINTY

GARY J. BALAS\*

*Department of Aerospace Engineering and Mechanics, University of Minnesota, Minneapolis, MN 55455, U.S.A.*

## SUMMARY

The structured singular value ( $\mu$ ) synthesis technique is used to design controllers for the Active Mass Damper (AMD) Benchmark problem. The motivation for using  $\mu$  synthesis is its ability to directly incorporate performance and robustness objectives into a multivariable control design framework. In addition to stated performance objectives, robustness of the controllers to high-frequency unmodelled dynamics (the neglected high-frequency modes of the evaluation model), modelling error in the actuator dynamics and variations in the first structural natural frequency and damping value are considered in the design. The resulting controller achieves similar performance levels on the nominal evaluation model and the evaluation model with significant variations in its first natural frequency and damping values. © 1998 John Wiley & Sons, Ltd.

KEY WORDS: robust control; structured singular value,  $\mu$ ; structural control

## 1. BENCHMARK PROBLEM: ACTIVE MASS DRIVER

The structured singular value ( $\mu$ ) framework is applied to the Active Mass Driver (AMD) benchmark problem describe in References 1 and 2. The objective is to actively control this three-storey, single-bay, scale model of a building. A single AMD actuator, located on the third floor of the structure, is used for control. The base of the structure is mounted to a shake table to simulate earthquake loadings. Six measurements are available for feedback: accelerometers at the base of the structure, on each storey, and on the actuator mass and an LVDT displacement sensor attached to the actuator.

The objective is to design a discrete-time feedback compensator that minimizes ten performance objectives. Five of the performance objectives correspond to minimizing rms responses of the structure and actuators. The other five performance objectives correspond to minimizing maximum displacements, accelerations and voltages. Two linear time-invariant models of the AMD structure are provided. The 10-state model is used for control design and the high-fidelity, 28-state evaluation model is used for analysis and simulation. The AMD benchmark problem does not directly include objectives or specifications on the robustness of the control design to modelling errors (model uncertainty). Using the 10-state AMD model for control design will require the controller to be robust (insensitive) to differences between the 28-state evaluation model and the 10-state design model. In addition to these neglected dynamics, the control design presented in this paper includes uncertainty models to account for actuator errors, sensor noise and variations in the damping value and natural frequency of the first structural mode.

---

\* Correspondence to: Gary J. Balas, Department of Aerospace Engineering and Mechanics, University of Minnesota, Minneapolis, MN 55455, U.S.A. E-mail: [balas@aem.umn.edu](mailto:balas@aem.umn.edu)

Contract/grant sponsor: National Science Foundation; Contract/grant number: CMS-9503370

## 2. THE STRUCTURED SINGULAR VALUE ( $\mu$ ) FRAMEWORK

Linear Fractional Transformations (LFTs) form the basis of the structured singular value ( $\mu$ ) framework. Figure 1 shows the standard control analysis and synthesis block diagrams. The  $\Delta$  block corresponds to structured perturbations or uncertainties and  $K$  corresponds to the controller. Any linear interconnection of inputs, outputs, commands, perturbations and controller can be rearranged to match these diagrams. The  $\mu$  framework allows the incorporation of knowledge of the modelling errors and performance objectives into the control analysis and design problem.

The structured singular value,  $\mu$ , is used to analyse linear fractional transformations when the  $\Delta$  block has structure. In the definition of  $\mu(M)$ , there is an underlying structure  $\Delta$  (a prescribed set of block diagonal matrices) on which everything in sequel depends. This structure may be defined differently for each problem depending on the uncertainty and performance objectives of the problem. Defining the structure involves specifying three things: the total number of blocks, the type of each block, and their dimensions.

### 2.1. The complex singular value

Two types of blocks—*repeated scalar* and *full* blocks are considered. Two nonnegative integers,  $S$  and  $F$ , denote the number of *repeated scalar* blocks and the number of *full* blocks, respectively. To bookkeep the block dimensions, we introduce positive integers  $r_1, \dots, r_S; m_1, \dots, m_F$ . The  $i$ th repeated scalar block is  $r_i \times r_i$ , while the  $j$ th full block is  $m_j \times m_j$ . With those integers given, define  $\Delta \subset \mathbf{C}^{n \times n}$ , complex square matrices, as

$$\Delta := \{\text{diag}[\delta_1 I_{r_1}, \dots, \delta_S I_{r_S}, \Delta_{S+1}, \dots, \Delta_{S+F}]: \delta_i \in \mathbf{C}, \Delta_{S+j} \in \mathbf{C}^{m_j \times m_j}, 1 \leq i \leq S, 1 \leq j \leq F\} \quad (1)$$

For consistency among all the dimensions, we must have  $\sum_{i=1}^S r_i + \sum_{j=1}^F m_j = n$ . Often, we will need norm bounded subsets of  $\Delta$ , and we introduce the notation  $\mathbf{B}_\Delta := \{\Delta \in \Delta: \sigma(\Delta) \leq 1\}$ . Note that in equation (1) all the repeated scalar blocks appear first, followed by the full blocks. This is done to simplify the notation and can easily be relaxed. The full blocks are also assumed to be square, but again, this is only to simplify notation.

*Definition 2.1.* For  $M \in \mathbf{C}^{n \times n}$ ,  $\mu_\Delta(M)$  is defined

$$\mu_\Delta(M) := \frac{1}{\min\{\bar{\sigma}(\Delta): \Delta \in \Delta, \det(I - M\Delta) = 0\}} \quad (2)$$

unless no  $\Delta \in \Delta$  makes  $I - M\Delta$  singular, in which case  $\mu_\Delta(M) := 0$ .

It is instructive to consider a ‘feedback’ interpretation of  $\mu_\Delta(M)$  at this point. Let  $M \in \mathbf{C}^{n \times n}$  be given, and consider the loop shown in Figure 2. This picture is meant to represent the loop equations  $u = Mv$ ,  $v = \Delta u$ . As long as  $I - M\Delta$  is nonsingular, the only solutions  $u, v$  to the loop equations are  $u = v = 0$ . However, if  $I - M\Delta$  is singular, then there are infinitely many solutions to the equations, and the norms  $\|u\|$ ,  $\|v\|$  of the solutions can be arbitrarily large. Motivated by connections with stability of systems, we call this constant

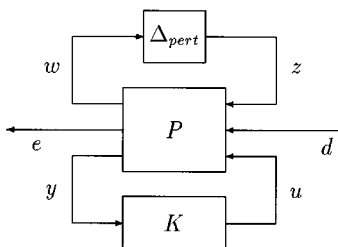
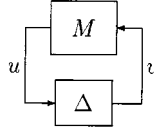


Figure 1. Linear fractional transformation description of control problem

Figure 2.  $M$ - $\Delta$  interconnection

matrix feedback system ‘unstable’. Likewise, the term ‘stable’ will describe the situation when the only solutions are identically zero. In this context then,  $\mu_\Delta(M)$  provides a measure of the smallest structured  $\Delta$  that causes ‘instability’ of the constant matrix feedback loop in Figure 2. The norm of this ‘destabilizing’  $\Delta$  is exactly  $1/\mu_\Delta(M)$ .

We can relate  $\mu_\Delta(M)$  to familiar linear algebra quantities when  $\Delta$  is one of two extreme sets:

- (a) If  $\Delta = \{\delta I: \delta \in \mathbf{C}\}$  ( $S = 1, F = 0, r_1 = n$ ), then  $\mu_\Delta(M) = \rho(M)$ , the spectral radius of  $M$ . The spectral radius is defined as the maximum magnitude eigenvalue of the matrix  $M$ .
- (b) If  $\Delta = \mathbf{C}^{n \times n}$  ( $S = 0, F = 1, m_1 = n$ ), then  $\mu_\Delta(M) = \bar{\sigma}(M)$ .

Obviously, for general  $\Delta$  as in equation (1) we must have  $\{\delta I_n: \delta \in \mathbf{C}\} \subset \Delta \subset \mathbf{C}^{n \times n}$ . Hence directly from the definition of  $\mu$ , and the two special cases above, we conclude that

$$\rho(M) \leq \mu_\Delta(M) \leq \bar{\sigma}(M) \quad (3)$$

These bounds by themselves may provide little information on the value of  $\mu$ , because the gap between  $\rho$  and  $\bar{\sigma}$  can be large. The bounds on  $\mu$  can be refined with transformation on  $M$  that do not affect  $\mu_\Delta(M)$ , but do affect  $\rho$  and  $\bar{\sigma}$ . To do this, define two subsets,  $\mathbf{Q}_\Delta$  and  $\mathbf{D}_\Delta$  of  $\mathbf{C}^{n \times n}$

$$\mathbf{Q}_\Delta = \{Q \in \Delta: Q^*Q = I_n\} \quad (4)$$

$$\mathbf{D}_\Delta = \left\{ \text{diag}[D_1, \dots, D_S, d_{S+1}I_{m_1}, \dots, d_{S+F}I_{m_F}]: \right. \\ \left. D_i \in \mathbf{C}^{r_i \times r_i}, D_i = D_i^* > 0, d_{S+j} \in \mathbf{R}, d_{S+j} > 0 \right\} \quad (5)$$

Note that for any  $\Delta \in \Delta$ ,  $Q \in \mathbf{Q}_\Delta$ , and  $D \in \mathbf{D}_\Delta$ ,

$$Q^* \in \mathbf{Q}_\Delta, \quad Q\Delta \in \Delta, \quad \Delta Q \in \Delta, \quad \bar{\sigma}(Q\Delta) = \bar{\sigma}(\Delta Q) = \bar{\sigma}(\Delta) \quad (6)$$

$$D\Delta = \Delta D \quad (7)$$

Therefore, the bounds in equation (3) can be tightened to

$$\max_{Q \in \mathbf{Q}} \rho(QM) \leq \max_{\Delta \in \mathbf{B}_\Delta} \rho(\Delta M) = \mu_\Delta(M) \leq \inf_{D \in \mathbf{D}} \bar{\sigma}(DMD^{-1}) \quad (8)$$

The lower bound,  $\max_{Q \in \mathbf{Q}} \rho(QM)$ , is actually always an equality.<sup>3</sup> Unfortunately, the quantity  $\rho(QM)$  can have multiple local maxima which are not global. Thus local search cannot be guaranteed to obtain  $\mu$ , but can only yield a lower bound. The upper bound can be reformulated as a convex optimization problem, so the global minimum can, in principle, be found. Unfortunately, the upper bound is not always equal to  $\mu$ . For block structures  $\Delta$  satisfying  $2S + F \leq 3$ , the upper bound is always equal to  $\mu_\Delta(M)$ , and for block structures with  $2S + F > 3$ , there exist matrices for which  $\mu$  is less than the infimum.<sup>3,4</sup>

## 2.2. The real complex structured singular value

Up until this point, this section has dealt with complex-valued perturbation sets. In specific instances, it may be more natural to describe modelling errors with real perturbations, for instance, when the real

coefficients of a linear differential equation are uncertain. While it is possible to simply treat these perturbations as complex and proceed with a complex  $\mu$  analysis, the results may be conservative. Hence, theory and algorithms to test for robustness and performance degradation with mixed (real blocks and complex blocks) perturbation have been developed.

Definition 2.1 (of  $\mu$ ) can be used for more general sets,  $\Delta$ , such as those containing real and complex blocks. Typically, there are three types of blocks—*repeated real scalar*, *repeated complex scalar*, and *complex full* blocks.  $S$  and  $F$ , denote the number of *repeated, complex scalar* blocks and the number of *complex full* blocks, respectively.  $V$  denotes the number of *repeated, real scalar* blocks. The block dimensions of the real block are denoted by the positive integers  $t_1, \dots, t_V$ . With these integers given, and  $r_i$  and  $m_j$ , define  $\Delta$  as

$$\Delta = \{\text{diag}[\delta_1^r I_{t_1}, \dots, \delta_V^r I_{t_V}, \delta_{V+1}^c I_{r_1}, \dots, \delta_{V+S}^c I_{r_S}, \Delta_{V+S+1}, \dots, \Delta_{V+S+F}]: \\ \delta_k^r \in \mathbf{R}, \delta_{V+i}^c \in \mathbf{C}, \Delta_{V+S+j} \in \mathbf{C}^{m_j \times m_j}, 1 \leq k \leq V, 1 \leq i \leq S, 1 \leq j \leq F\} \quad (9)$$

For consistency among all the dimensions, we must have  $\sum_{k=1}^V t_k + \sum_{i=1}^S r_i + \sum_{j=1}^F m_j = n$ . The mixed  $\mu$  function inherits many of the properties of the purely complex  $\mu$  function.<sup>3,5</sup> The theory for bounding (both lower and upper) mixed real/complex bounds is much more complicated to describe than the bounding theory for complex  $\mu$ . The lower bound for the mixed case is a real eigenvalue maximization problem. Techniques for approximately solving for a mixed  $\mu$  lower bound using power algorithms have been derived, and are similar to those used for a lower bound for complex  $\mu$ .<sup>6</sup> The mixed  $\mu$  upper bound takes the form of a more complicated version of the same problem, involving an additional ‘ $G$  scaling matrix’ which only scales the real uncertainty blocks.

### 2.3. Linear fractional transformations and $\mu$

The use of  $\mu$  in control theory depends to a great extent on its intimate relationship with a class of general linear feedback loops called Linear Fractional Transformations (LFTs).<sup>7</sup> This section explores this relationship with some simple theorems that can be obtained almost immediately from the definition of  $\mu$ . To introduce these, consider a complex matrix  $M$  partitioned as

$$M = \begin{bmatrix} M_{11} & M_{12} \\ M_{21} & M_{22} \end{bmatrix} \quad (10)$$

and suppose there is a defined block structure  $\Delta_1$  which is compatible in size with  $M_{11}$  (for any  $\Delta_1 \in \Delta_1$ ,  $M_{11}\Delta_1$  is square). For  $\Delta_1 \in \Delta_1$ , consider the loop equations

$$z = M_{11}w + M_{12}d, \quad e = M_{21}w + M_{22}d, \quad w = \Delta_1 z \quad (11)$$

which correspond to the block diagram in Figure 3.

This set of equations (11) is called well posed if for any vector  $d$ , there exist unique vectors  $w$ ,  $z$ , and  $e$  satisfying the loop equations. The set of equations is well posed if and only if the inverse of  $I - M_{11}\Delta_1$  exists. If not, then depending on  $d$  and  $M$ , there is either no solution to the loop equations, or there are an infinite number of solutions. When the inverse does indeed exist, the vectors  $e$  and  $d$  must satisfy  $e = F_u(M, \Delta_1)d$ , where

$$F_u(M, \Delta_1) := M_{22} + M_{21}\Delta_1(I - M_{11}\Delta_1)^{-1}M_{12} \quad (12)$$

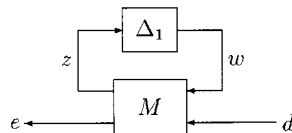


Figure 3. Linear fractional transformation

$F_u(M, \Delta_1)$  is called a LFT on  $M$  by  $\Delta_1$ , and in a feedback diagram appears as shown in Figure 3.  $F_u(M, \Delta_1)$  denotes that the 'upper' loop of  $M$  is closed by  $\Delta_1$ . An analogous formula describes  $F_\ell(M, \Delta_2)$  which is the resulting matrix obtained by closing the 'lower' loop of  $M$  with a matrix  $\Delta_2 \in \Delta_2$ .

In this formulation, the matrix  $M_{22}$  is assumed to be something nominal, and  $\Delta_1 \in \mathbf{B}_{\Delta_1}$  is viewed as a norm bounded perturbation from an allowable perturbation class,  $\Delta_1$ . The matrices  $M_{12}$ ,  $M_{21}$ , and  $M_{22}$  and the formula  $F_u(M, \Delta_1)$  reflect prior knowledge on how the unknown perturbation affects the nominal map,  $M_{22}$ . This type of uncertainty, called *linear functional*, is natural for many control problems, and encompasses many other special cases considered by researchers.

### 3. CONTROL DESIGN VIA $\mu$ SYNTHESIS

Consider the standard linear fractional description of the control problem show in Figure 1. The  $P$  block represents the open-loop interconnection and contains all of the known elements including the nominal plant model, uncertainty structure and performance and uncertainty weighting functions. The  $\Delta_{\text{pert}}$  block represents the structured set of norm bounded uncertainty being considered and  $K$  represents the controller.  $\Delta_{\text{pert}}$  parametrizes all of the assumed model uncertainty in the problem. Three groups of inputs enter  $P$ , perturbations  $z$ , disturbances  $d$ , and controls  $u$ , and three groups of outputs are generated, perturbations  $w$ , errors  $e$  and measurements  $y$ . The set of systems to be controlled is described by the LFT

$$\{F_u(\Delta_{\text{pert}}, P) : \Delta_{\text{pert}} \in \mathbf{S}_{\Delta_{\text{pert}}}\},$$

The design objective is to achieve 'robust performance'. That is find a stabilizing controller  $K$ , such that for all  $\Delta_{\text{pert}} \in \mathbf{S}_{\Delta_{\text{pert}}}$ ,  $\|\Delta_{\text{pert}}\|_\infty \leq 1$ , the closed-loop system is stable and satisfies

$$\|F_u[F_\ell(P, K), \Delta_{\text{pert}}]\|_\infty \leq 1.$$

The performance objective involves a robust performance test on the linear fractional transformation  $F_\ell(P, K)$ . Achieving robust performance implies that the performance objective is achieved for *all* plant defined by the model set  $F_u(P, \Delta_{\text{pert}})$ . To assess the robust performance of the close-loop system, define an augmented perturbation structure,  $\Delta$ ,

$$\Delta = \left\{ \begin{bmatrix} \Delta_{\text{pert}} & 0 \\ 0 & \Delta_F \end{bmatrix} : \Delta_{\text{pert}} \in \Delta_{\text{pert}}, \Delta_F \in \mathbf{C}^{n_d \times n_e} \right\}$$

The goal of  $\mu$  synthesis is to minimize over all stabilizing controllers  $K$ , the peak value of  $\mu_\Delta(\cdot)$  of the closed-loop transfer function  $F_\ell(P, K)$  across frequency  $\omega$ . This corresponds exactly with achieving robust performance for the generalized model  $P$ . More formally,

$$\min_{\substack{K \\ \text{stabilizing}}} \max_{\omega} \mu_\Delta[F_\ell(P, K)(j\omega)] \quad (13)$$

For tractability of the  $\mu$  synthesis problem,  $\mu_\Delta[\cdot]$  is replaced by the upper bound for  $\mu$ ,  $\bar{\sigma}[D(\cdot)D^{-1}]$ . The scaling matrix  $D$  is a member of the appropriate set of scaling matrices  $\mathbf{D}$  for the perturbation set  $\Delta$ . One can reformulate this optimization problem as follows:

$$\min_{\substack{K \\ \text{stabilizing}}} \max_{\omega} \min_{D_\omega \in \mathbf{D}} \bar{\sigma}[D_\omega F_\ell(P, K)(j\omega) D_\omega^{-1}] \quad (14)$$

Here, the  $D$  minimization is an approximation to the  $\mu_\Delta[F_\ell(P, K)(j\omega)]$ .  $D_\omega$  is chosen from the set of scalings,  $\mathbf{D}$ , independently at every frequency  $\omega$ . Hence, we have

$$\min_{\substack{K \\ \text{stabilizing}}} \min_{\substack{D_{(\cdot)} \\ D_\omega \in \mathbf{D}}} \max_{\omega} \bar{\sigma}[D_\omega F_\ell(P, K)(j\omega) D_\omega^{-1}] \quad (15)$$

The expression  $\max_{\omega} \bar{\sigma}[\cdot]$  corresponds to  $\|\cdot\|_{\infty}$ , leaving

$$\min_{\substack{K \\ \text{stabilizing}}} \min_{\substack{D_{\omega} \\ D_{\omega} \in \mathbf{D}}} \| [D_{\omega} F_{\ell}(P, K)(j\omega) D_{\omega}^{-1}] \|_{\infty} \quad (16)$$

Assume, for simplicity, that the uncertainty block  $\mathbf{A}_{\text{pert}}$  only has full blocks. Then the set  $\mathbf{D}_{\mathbf{A}}$  is of the form

$$\mathbf{D} = \{\text{diag}[d_1 I, d_2 I, \dots, d_{F-1} I, I]: d_i > 0\} \quad (17)$$

For any complex matrix  $M$ , the elements of  $\mathbf{D}_{\mathbf{A}}$ , which were originally defined to be real and positive, can actually take on any non-zero complex values and not change the value of the upper bound,  $\inf_{D \in \mathcal{D}} \bar{\sigma}(DMD^{-1})$ . Hence, we can restrict the scaling matrix to be a real-rational, stable, minimum-phase transfer function,  $\hat{D}(s)$ . The optimization is now

$$\min_{\substack{K \\ \text{stabilizing}}} \min_{\substack{\hat{D}(s) \in \mathbf{D} \\ \text{stable, min-phase}}} \| [\hat{D} F_{\ell}(P, K) \hat{D}^{-1}] \|_{\infty} \quad (18)$$

This approximation to  $\mu$ -synthesis, is currently ‘solved’ by an iterative approach, referred to as ‘ $D$ – $K$  iteration’.

To solve equation (18), first consider holding  $\hat{D}(s)$  fixed. Given a stable, minimum phase, real-rational  $\hat{D}(s)$ , solved the optimization

$$\min_{\substack{K \\ \text{stabilizing}}} \| [\hat{D} F_{\ell}(P, K) \hat{D}^{-1}] \|_{\infty}$$

This equation is an  $\mathcal{H}_{\infty}$  optimization control problem. The solution to the  $\mathcal{H}_{\infty}$  problem is well known and consists of solving algebraic Riccati equations in terms of the state-space system.<sup>8</sup>

Now suppose that a stabilizing controller,  $K(s)$ , is given, we then solve the following minimization corresponding to the upper bound for  $\mu$ :

$$\min_{D_{\omega} \in \mathbf{D}} \bar{\sigma}[D_{\omega} F_{\ell}(P, K)(j\omega) D_{\omega}^{-1}]$$

This minimization is done over the real, positive  $D_{\omega}$  from the set  $\mathbf{D}_{\mathbf{A}}$  defined in equation (17) across frequency  $\omega$ . Recall that the addition of phase to each  $d_i$  does not affect the value of  $\bar{\sigma}[D_{\omega} F_{\ell}(P, K)(j\omega) D_{\omega}^{-1}]$ . Hence, each discrete function  $d_i$ , of frequency is fit (in magnitude) by a proper, stable, minimum-phase transfer function,  $\hat{d}_{R_i}(s)$ . These are collected together in a diagonal transfer function matrix  $\hat{D}(s)$ ,

$$\hat{D}(s) = \text{diag}[\hat{d}_{R_1}(s)I, \hat{d}_{R_2}(s)I, \dots, \hat{d}_{R_{F-1}}(s)I, I]$$

and absorbed into the original open-loop generalized plant  $P$ . Iterating on these two steps comprises the current approach to  $D$ – $K$  iteration.

There are several problems with the  $D$ – $K$  iteration control design procedure. The first is that we have approximated  $\mu_{\mathbf{A}}(\cdot)$  by its upper bound. This is not a serious problem since the value of  $\mu$  and its upper bound are often close. The most serious problem is that the  $D$ – $K$  iteration does not always converge to a global, or even local minimum.<sup>9</sup> This is a more severe limitation of the design procedure. However, in practice the  $D$ – $K$  iteration control design technique appears to work very well on many engineering problems and has been applied with great success to vibration suppression for flexible structures, flight control, chemical process control problems, and acoustic reverberation suppression in enclosures.

#### 4. CONTROL PROBLEM FORMULATION

The structured singular value ( $\mu$ ) synthesis technique is used for controller design.<sup>4,8,10–12</sup> The key to successfully applying  $\mu$ -synthesis is in the formulation of the control design problem. That is all robustness and performance objectives need to be posed as minimizing the norm of weight transfer function(s). All

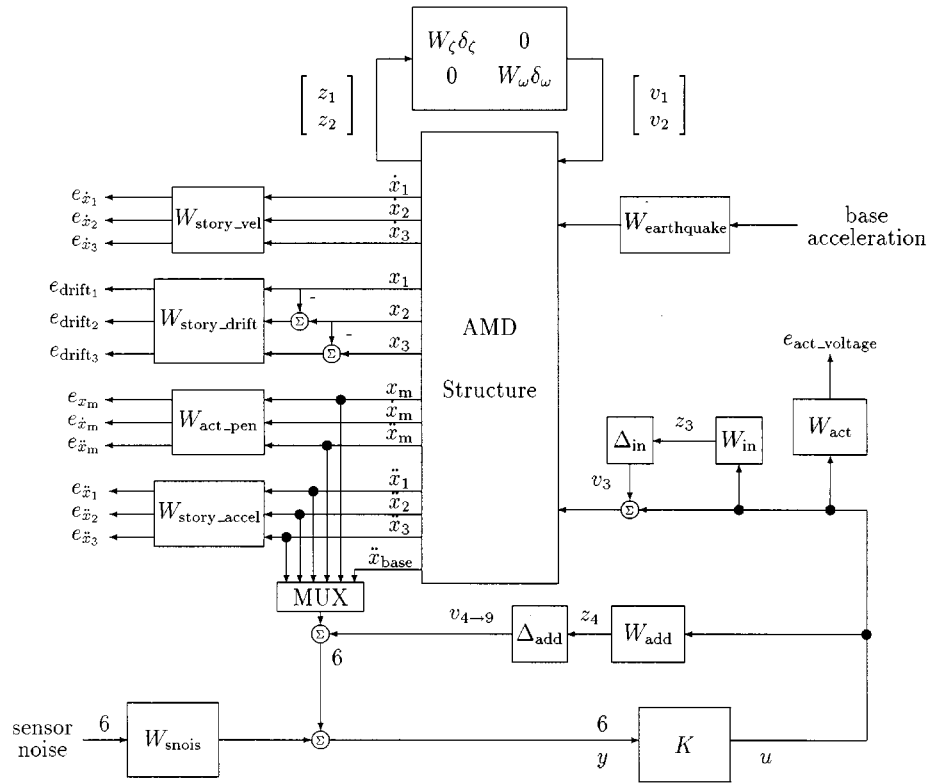


Figure 4. Interconnection structure of the AMD control problem

uncertainty models need to be normalized to magnitude less than 1 in the  $\mu$  framework. In this example, this implies that the weighting functions  $W_\zeta$ ,  $W_\omega$ ,  $W_{in}$ , and  $W_{add}$  need to be scaled such that  $|\delta_\zeta|$ ,  $|\delta_\omega|$ ,  $|\Delta_{in}|$ , and  $|\Delta_{add}|$  are less than 1. The performance objectives are defined in terms of minimizing the  $\mathcal{H}_\infty$  norm of a weighted transfer matrix from disturbances (**d**) to errors (**e**) denoted as  $T_{d \rightarrow e}$ . As in the robustness to modelling errors formulation, the performance weighting functions are scaled such that when  $\|T_{d \rightarrow e}\|_\infty$  is less than 1 all performance objectives are achieved. The AMD control problem is posed as a robust performance problem, with multiplicative plant uncertainty at the plant input, additive uncertainty around the plant, parametric uncertainty in the natural frequency and damping value of the first mode and minimization of weighted error transfer functions as the performance criterion.<sup>12</sup> The actuator voltage, displacement, velocity, and acceleration signals are weighted to insure that they do not exceed their physical capabilities. Sensor noise is included on the six measurements to mimic the experimental system. The performance objectives are included as minimizing weighted transfer functions associated with storey velocities and accelerations and inter-storey displacements. A diagram of the system interconnection structure used for control design and analysis is shown in Figure 4. Based on Figure 4, the generalized plant  $P$  used for control design is shown in Figure 5.

Note that the state order of the  $\mu$  controller is the sum of the number of states in the generalized plant  $P$  plus twice the number of states in the  $D$  scaling matrices. Since it is often desired to synthesize low-order controllers, the lowest-order weighting functions that adequately describe the objectives are used. In this application, all the weights are constant except for  $W_{add}$  and  $W_{earthquake}$ .

The performance objective is to have the 'true' structure, described by the control design and uncertainty models, achieve the desired performance objectives. Note that these models define a much richer set of

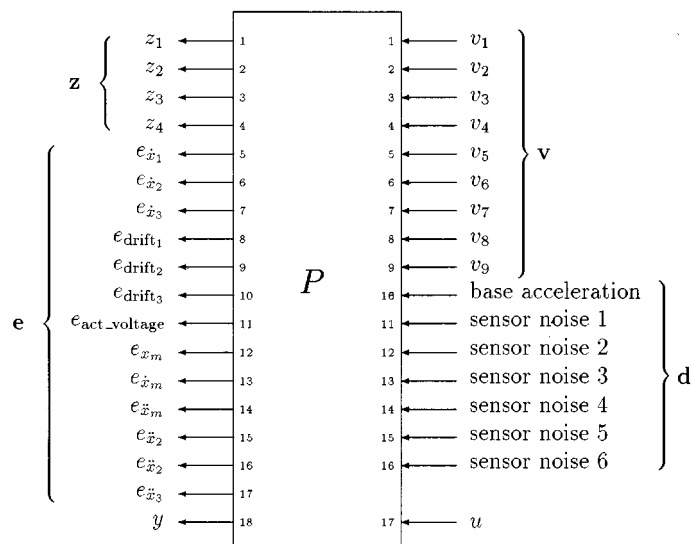


Figure 5. Generalized plant for the AMD control problem

structural systems than just the evaluation model. The evaluation model is included in this set of models to be controlled, but also included in this set are structures that have *different* natural frequency and damping values of the first structural mode, different actuator gain and phase characteristics and additional high-frequency dynamics.

The Benchmark performance objectives are entirely driven by the ability of the controller to attenuate the response of the first mode of the AMD structure and the actuator accelerator limit. Therefore, only the inter-storey drift and the storey accelerations need to be heavily penalized in the control design. The performance weighting functions in Figure 4 are defined as follows:

- (i)  $W_{\text{earthquake}}$  defined as

$$\frac{0.00036s^3 + 32.1s^2 + 66000s + 14400}{s^3 + 1000s^2 + 75400s + 276000}$$

is used to describe the square-root of the Kanai–Tajmi earthquake spectra. A frequency response plot of this weight is shown in Figure 6.  $W_{\text{earthquake}}$  models the frequency spectra of a general earthquake.

- (ii)  $W_{\text{act}}$  weights to actuator control voltage input. It is selected to be 0.4. This corresponds to a maximum of 2.5 V being commanded to the actuator. The error signal  $e_{\text{act\_voltage}}$  being less than 1 implies that less than 2.5 v are being commanded to the actuator.  $W_{\text{snos}}$  is a  $6 \times 6$  matrix with 0.001 in its diagonal entries. These are estimate of the sensor noise levels.
- (iii)  $W_{\text{storey\_vel}}$ ,  $W_{\text{storey\_drift}}$ , and  $W_{\text{storey\_accel}}$  are  $3 \times 3$  matrices with diagonal entries of (0.04, 0.025, 0.021), (0.06, 0.10, 0.23), and (0.011, 0.007, 0.006), respectively. These weights are selected to attenuate the response of the first mode in the control design. Each scaling was selected such that the transfer function from base acceleration input to the corresponding output (i.e. storey\_vel, storey\_drift, and storey\_accel) have a peak magnitude of 3 at the first mode of the AMD structure. Therefore, if robust performance is achieved, the response of the first mode would be approximately attenuated by a factor of 3 in each channel. If the response of one channel is more important than other channels, the user would put a large scaling on the important channel as compared with the less important channels.



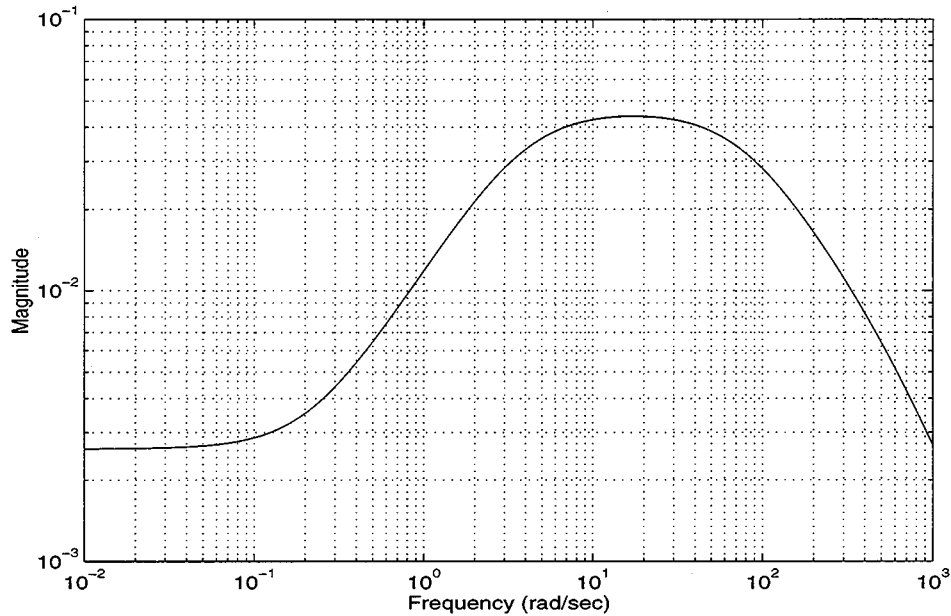


Figure 6. Frequency response of the Kanai-Tajimi earthquake spectra,  $W_{\text{earthquake}}$

- (iv)  $W_{\text{act\_pen}}$  is a  $3 \times 3$  matrix with a diagonal entries of 0.04, 0.03, 0.002, respectively. Since the transfer functions between the actuator input and its displacement, velocity and acceleration are related and only the first mode plays a role in the performance objectives, only the actuator displacement output is heavily weighted. As discussed previously, each individual transfer function is scaled such that the constraints on the actuator displacement, velocity and acceleration are not violated.
- (v)  $W_{\text{in}}$  is set to 0.1 corresponding to 10 per cent uncertainty in the actuator response.
- (vi) The additive uncertainty weight,  $W_{\text{add}}$ , is defined as

$$\frac{11.4s^2 + 162s + 917}{s^2 + 103s + 17206}$$

$W_{\text{add}}$  accounts for differences in the second and third modes of the control design and evaluation models as well as high-frequency dynamics in the evaluation model that were not included in the control design model. The shape of the additive uncertainty weight is selected to gain-stabilize the neglected evaluation model dynamics. To achieve this objective,  $W_{\text{add}}$  is shaped to limit the controller gain at high frequency. In the problem formulation, if robust performance is achieved the controller gain at high frequency will be less than the inverse of the additive uncertainty weight. Hence the loop gain at high frequency will be less than 1, gain-stabilizing the neglected dynamics of the system. A frequency response plot of  $W_{\text{add}}$  and the difference between the control design and evaluation model is shown in Figure 7. Note that  $W_{\text{add}}$  over bounds the difference between the control design and evaluation model to assure that the neglected dynamics are not destabilized.

- (vii)  $W_{\zeta}$  is set to 0.5 or 50 per cent error in the damping level of the first mode. A benefit of directly designing for uncertainty in the level of damping using  $D$ - $K$  iteration is it results in robustness to variations in the first structural mode.<sup>12</sup>  $W_{\omega}$  is set to zero in the control design and set to 0.25 (12 per cent) error in the natural frequency of the first mode in the analysis.

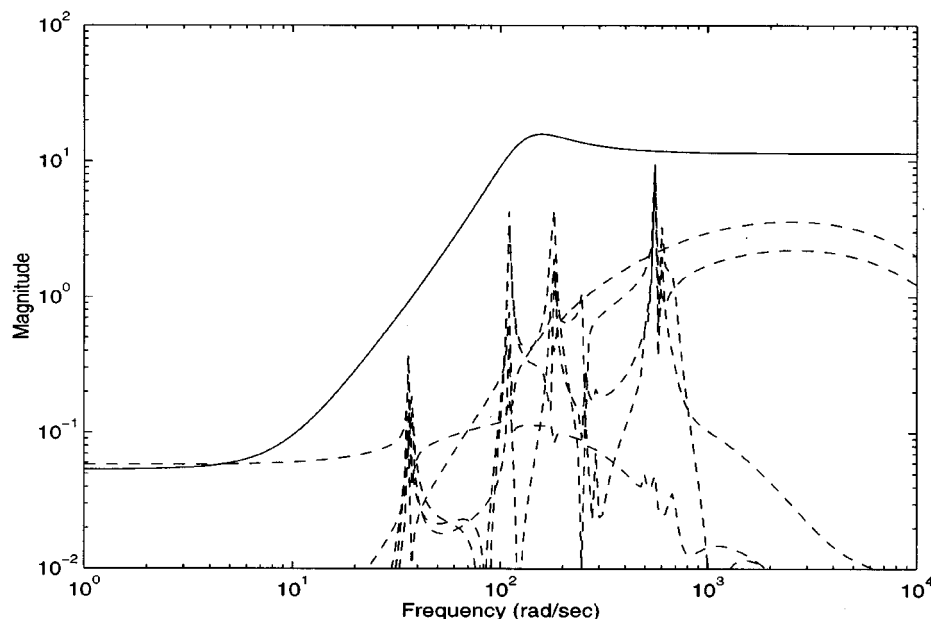


Figure 7. Frequency response of the additive uncertainty weight,  $W_{\text{add}}$  (solid), and errors between the design and evaluation models (dashed)

Weighting functions serve two purposes in the  $\mathcal{H}_\infty$  and  $\mu$  framework: they allow the direct comparison of different performance objectives with the same norm and they allow frequency information to be incorporated into the analysis. All the weighted performance objectives are scaled to have an  $\mathcal{H}_\infty$  less than 1 when they are achieved.<sup>11</sup>

The approach taken to synthesize a discrete-time controller sampled at 1000 Hz for the AMD structure is to synthesize a continuous-time controller via  $D$ - $K$  iteration and discretize it using a pre-warped Tustin transformation. This approach was taken since a closed-loop bandwidth of approximately 80 rad/sec was desired, a factor of 30 less than the Nyquist sample rate. Therefore, the effect of discretizing a continuous-time controller is small. Alternatively, one could directly propose this problem in discrete-time and synthesize a controller using  $D$ - $K$  iteration.<sup>11</sup>

## 5. RESULTS

Three  $D$ - $K$  iterations are performed to design a  $\mu$  continuous-time controller. The original interconnections structure  $P$  in Figures 5 has 14 states. The  $D$  scaling matrix after 3 iterations has 7 states. Therefore, the resulting  $\mu$  controller has 28-state ( $14 + 7 + 7$ ). The balanced realization method was used to reduced the controller order to 12-states which is used in the analysis and simulations.

The robust performance and robust stability  $\mu$  value of the closed-loop system with the 12-state controller implemented, and the natural frequency and damping value treated as real perturbations were 0.87, respectively, as seen in Figures 8 and 9. Since the performance and robustness objectives were scaled to be 1 when they were achieved and since the robust performance  $\mu$  value is less than 1 (0.87), all performance and robustness objectives were achieved simultaneously. The robust performance  $\mu$  value with the natural frequency and damping value treated as complex perturbations is 3.4 as seen in Figure 8. Since  $\mu$  is greater than 1 (3.4) in this case, treating the natural frequency and damping uncertainties as complex perturbations in the analysis of the closed-loop system, as opposed to real parameter variation, would be overly conservative. The nominal performance value was 0.2. Hence if no model error was present, all the

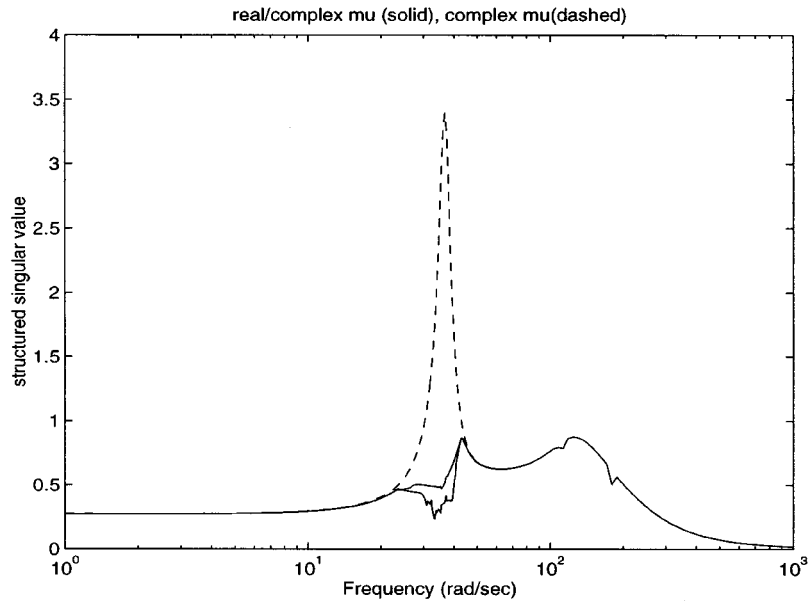


Figure 8. Mixed real/complex robust performance (solid) and complex robust performance (dashed) plots

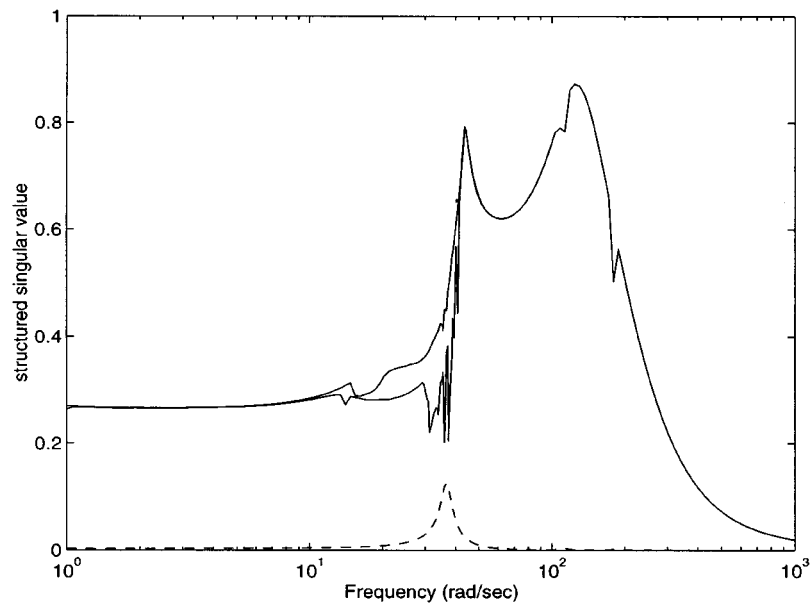


Figure 9. Robust stability (solid) and nominal performance (dashed) plots

performance objectives would be achieved. Based on nominal performance, robust stability and robust performance results, the control design was driven by satisfying the robustness objectives.

Note that in Figures 8 and 9 there are two solid lines. These lines correspond to upper and lower bounds on  $\mu$ . The  $\mu$  software used calculates upper and lower bounds for  $\mu$  to provide a measure of accuracy of the  $\mu$  calculations.<sup>11</sup>

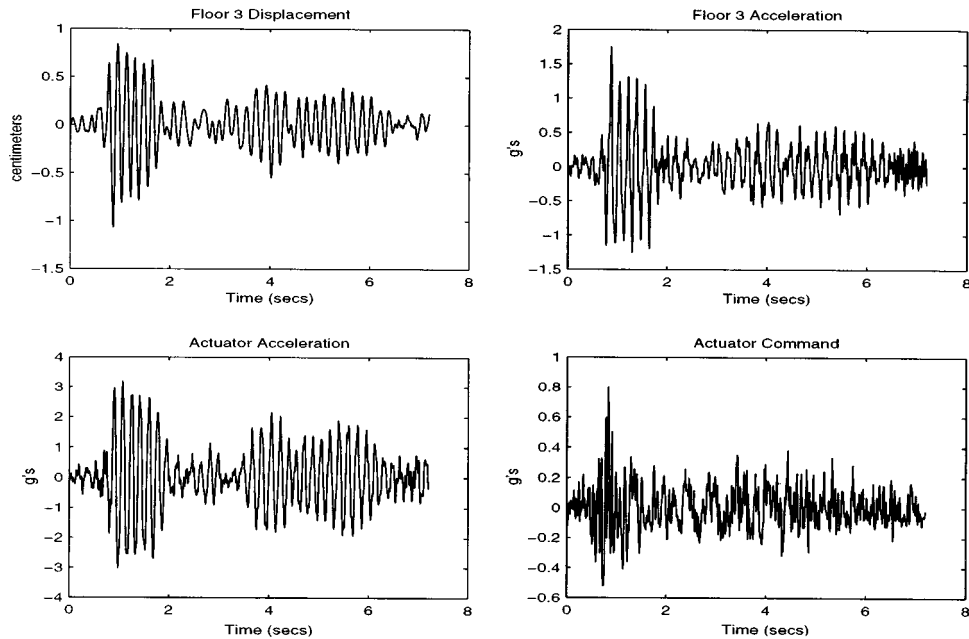


Figure 10. Nominal time response to Hachinohe earthquake spectrum

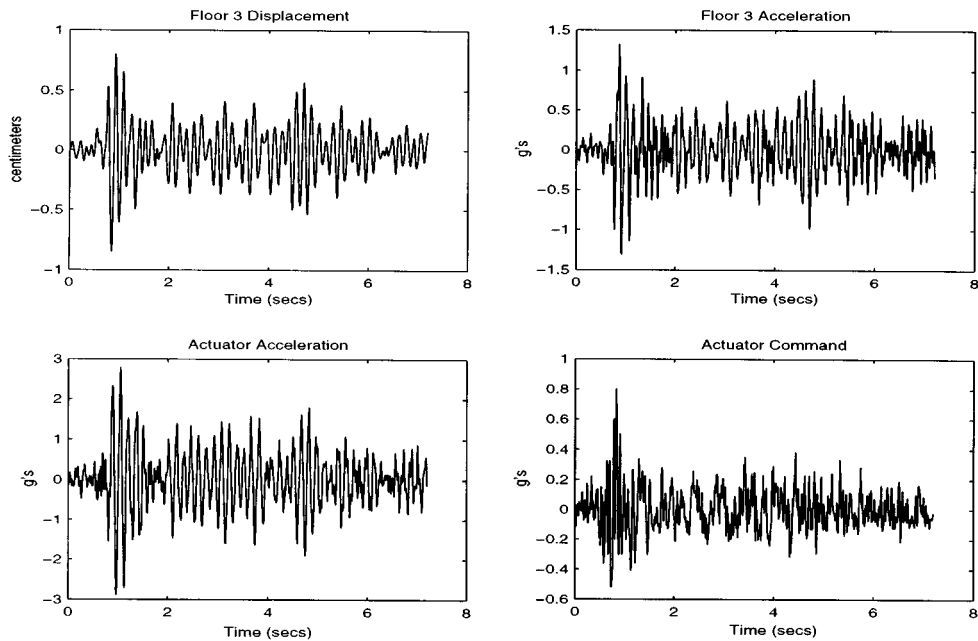


Figure 11. Perturbed time response to Hachinohe earthquake spectrum

The  $\mu$  robust performance analysis test determined that the worst-case variation from a performance and stability perspective was to perturb the first natural frequency from 36.51 to 41.42 rad/sec and its damping value from 0.34 to 0.22%. To investigate the effect of these changes in natural frequency and damping value,

Table I. Nominal and perturbed performance measures

	El Centro		Hachinohe	
	Nominal model	Perturbed	Nominal model	Perturbed
J6	0.3122	0.2588	0.3778	0.3366
J7	0.4790	0.4711	0.6791	0.5258
J8	1.2670	0.9413	1.4289	1.1931
J9	1.2141	0.9922	1.5374	1.3274
J10	1.0951	0.8227	1.2368	1.1174
max act volt	1.191	0.918	0.661	0.571
max act disp	4.270	3.172	2.372	1.981
max act accel	5.530	4.155	3.191	2.883

two sets of simulations are performed. The first uses the original evaluation model as the plant model. The second simulation perturbs the natural frequency of the first structural mode from 36.51 to 41.42 rad/sec and its damping ratio from 0.34 to 0.22% damping. Time responses of the third-storey displacement and acceleration, the actuator mass acceleration and command voltage for the nominal and perturbed structural models subjected to the Hachinohe earthquake spectrum are shown in Figures 10 and 11.

There are 10 performance indices, denoted J1–J10, associated with the AMD benchmark example. J1–J5 correspond to the rms response of the AMD excited by a stationary random process filtered through the Kanai–Tajimi spectrum. J1 corresponds to the normalized maximum rms inter-storey drift, J2 the normalized maximum rms storey acceleration, and J3–J5 correspond to the normalized maximum rms actuator displacement, velocity and acceleration. J6–J10 are performance indices associated with the peak response due to the 1940 El Centro NS earthquake record and the 1968 Hachinohe NS earthquake record. J6 corresponds to the normalized maximum inter-storey drift, J7 the normalized maximum storey acceleration, and J7–J10 correspond to the normalized maximum actuator displacement, velocity and acceleration.

Table I contains the J6–J10 performance indices for the nominal and perturbed evaluation models with the 12-state discrete-time controller implemented. Based on the results in Figures 10 and 11 and Table I, the  $\mu$  controller is robust to variations in the first mode natural frequency and damping value and performs well. The value of J1–J5 with  $w_g = 37.3$  rad/sec and  $\zeta_g = 0.3$  for the nominal evaluation model are (0.91, 0.293, 0.841, 0.836, 0.813) respectively. Based on these results,  $\mu$  synthesis was able to design a controller which achieved good performance on the AMD structure in the presence of modeling error.

#### ACKNOWLEDGEMENTS

The author wishes to acknowledge the financial support from the NSF Structural Control Research for Performance, Safety and Hazard Mitigation Program (CMS-9503370) and would like to thank Jon Andersh, Petros Tratskas, and Lance Beall for their control designs of the AMD structure. The author also would like to thank the reviewers for their helpful comments.

#### REFERENCES

1. S. J. Dyke, B. F. Spencer Jr., A. E. Belknap, K. J. Ferrell, P. Quast and M. K. Sain, 'Absolute acceleration feedback control strategies for the active mass driver', *Proc. First World Conf. on Structural Control*, Vol. 2, Pasadena, CA, August 3–5 1994, pp. TP1:51–TP1:60.
2. B. F. Spencer Jr., S. J. Dyke and H. S. Deoskar, 'Benchmark problems in structural control, Part I: Active mass driver System', *Proc. 1997 ASCE Structures Congress*, Portland, OR, 13–16 April 1997.
3. J. C. Doyle, 'Analysis of feedback systems with structured uncertainties', *IEEE Proc. Part D* **129**, 242–250 (1982).
4. A. K. Packard and J. Doyle, 'The complex structured singular value', *Automatica* **29**, 71–109 (June 1993).
5. M. Fan, A. Tits and J.-C. Doyle, 'Robustness in the presence of joint parametric uncertainty and unmodeled dynamics', *IEEE Trans. Automat. Control* **36**, 25–38 (1991).

6. P. M. Young, M. P. Newlin and J. C. Doyle, ' $\mu$  analysis with real parametric uncertainty', in *Proc. 30th IEEE Conf. on Decision and Control*, Hawaii, 1991, pp. 1251–1256.
7. Redheffer, 'On a certain linear fractional transformation', *Journal of Mathematics and Mechanics* **8**(3), (1959).
8. J. C. Doyle, K. Glover, P. P. Khargonekar and B. A. Francis, 'State-space solutions to standard  $H_2$  and  $H_\infty$  control problems', *IEEE Trans. Automat. Control* **AC-34**, 831–8447 (1989); *J. Math. Phys.* **39**, 269–286 (1960).
9. G. Stein and J. C. Doyle, 'Beyond singular values and loopshapes', *AIAA J. Guidance Control* **14**(1), 5–16 (1991).
10. A. K. Packard, J. C. Doyle and G. J. Balas, 'Linear, multivariable robust control with a  $\mu$  perspective', *ASME J. Dyn. Measurements and Control Special Edition on Control* **115**(2), 426–438 (1993).
11. G. J. Balas, J. C. Doyle, K. Glover, A. K. Packard and R. Smith,  *$\mu$ -Analysis and Synthesis Toolbox: User's Guide*, MUSYN Inc. and The Mathworks Inc., December, 1990.
12. G. J. Balas and P. M. Young, 'Control design for variations in structural natural frequencies', *AIAA J. Guidance, Dyn. Control* **18**(2), 325–332 (1995).